

NASA TECHNICAL MEMORANDUM

NASA TM X-64646

PASSIVE STABILITY OF A SPINNING SKYLAB

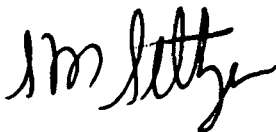
By S. M. Seltzer
Astrionics Laboratory

CASE FILE
COPY

February 25, 1972

NASA

*George C. Marshall Space Flight Center
Marshall Space Flight Center, Alabama*

1. REPORT NO. TM X 64646		2. GOVERNMENT ACCESSION NO.		3. RECIPIENT'S CATALOG NO.	
4. TITLE AND SUBTITLE Passive Stability of a Spinning Skylab				5. REPORT DATE February 25, 1972	
				6. PERFORMING ORGANIZATION CODE	
7. AUTHOR(S) S. M. Seltzer				8. PERFORMING ORGANIZATION REPORT NO.	
9. PERFORMING ORGANIZATION NAME AND ADDRESS George C. Marshall Space Flight Center Marshall Space Flight Center, Alabama 35812				10. WORK UNIT NO.	
				11. CONTRACT OR GRANT NO.	
12. SPONSORING AGENCY NAME AND ADDRESS National Aeronautics and Space Administration Washington, D.C. 20546				13. TYPE OF REPORT & PERIOD COVERED Technical Memorandum	
				14. SPONSORING AGENCY CODE	
15. SUPPLEMENTARY NOTES Prepared by Astrionics Laboratory, Science and Engineering Directorate					
16. ABSTRACT <p>The results of an analytical investigation of the rotational dynamics of a spinning Skylab space station are presented. The passive stability of motion of a simplified model consisting of a rigid core body with two attached flexible appendages is investigated. The parameter plane stability technique is applied to the specific Skylab case to determine its transient response to external disturbances.</p>					
17. KEY WORDS Stability Spinning body dynamics Flexible spinning body dynamics Parameter plane technique			18. DISTRIBUTION STATEMENT <p>Unclassified - Unlimited</p> 		
19. SECURITY CLASSIF. (of this report) Unclassified		20. SECURITY CLASSIF. (of this page) Unclassified		21. NO. OF PAGES 22	
				22. PRICE \$ 3.00	

ACKNOWLEDGMENT

The author gratefully acknowledges the advice of Dr. Jayant Patel, Principal Engineer with Teledyne-Brown Engineering Company, Huntsville, Alabama.

TECHNICAL REPORT STANDARD TITLE PAGE			
1. REPORT NO. TM X 64646	2. GOVERNMENT ACCESSION NO.	3. RECIPIENT'S CATALOG NO.	
4. TITLE AND SUBTITLE Passive Stability of a Spinning Skylab		5. REPORT DATE February 25, 1972	6. PERFORMING ORGANIZATION CODE
7. AUTHOR (S) S. M. Seltzer		8. PERFORMING ORGANIZATION REPORT #	
9. PERFORMING ORGANIZATION NAME AND ADDRESS George C. Marshall Space Flight Center Marshall Space Flight Center, Alabama 35812		10. WORK UNIT NO.	11. CONTRACT OR GRANT NO.
12. SPONSORING AGENCY NAME AND ADDRESS National Aeronautics and Space Administration Washington, D. C. 20546		13. TYPE OF REPORT & PERIOD COVERED Technical Memorandum	
14. SPONSORING AGENCY CODE			
15. SUPPLEMENTARY NOTES Prepared by Astrionics Laboratory, Science and Engineering Directorate			
16. ABSTRACT The results of an analytical investigation of the rotational dynamics of a spinning Skylab space station are presented. The passive stability of motion of a simplified model consisting of a rigid core body with two attached flexible appendages is investigated. The parameter plane stability technique is applied to the specific Skylab case to determine its transient response to external disturbances.			
17. KEY WORDS Stability Spinning body dynamics Flexible spinning body dynamics Parameter plane technique		18. DISTRIBUTION STATEMENT Unclassified - Unlimited <i>sm seltzer</i>	
19. SECURITY CLASSIF. (of this report) Unclassified	20. SECURITY CLASSIF. (of this page) Unclassified	21. NO. OF PAGES 22	22. PRICE \$ 3.00

TABLE OF CONTENTS

	Page
INTRODUCTION	1
MODEL DEFINITION AND EQUATIONS OF MOTION	1
STABILITY ANALYSIS	4
WOBBLE MOTION DYNAMICS	7
CONCLUSION	13
REFERENCES	16

LIST OF ILLUSTRATIONS

Figure	Title	Page
1.	Skylab	2
2.	Simplified model	2
3.	Stability region for wobble motion	6
4.	Stability region for in-plane motion	8
5.	K_2 versus K_1K_2 parameter plane plot	12
6.	w_1 versus τ	14
7.	w_2 versus τ	14
8.	μ_3 versus τ	15

LIST OF TABLES

Table	Title	Page
1.	Coefficients of Wobble Characteristic Equation	9
2.	Physical Characteristics of Skylab	11

PASSIVE STABILITY OF A SPINNING SKYLAB

INTRODUCTION

In 1970 NASA's Marshall Space Flight Center initiated a study to determine the feasibility of spinning the Skylab (the first U.S. manned orbiting space station). The purpose of the spin would be to provide artificial gravity so that its effects might be assessed. One facet of this study is presented in this paper.

In spinning the Skylab, it would be necessary to point the solar panels toward the sun. This would require the vehicle to spin about a principal axis of intermediate moment of inertia, which cannot be done stably. That axis can be made the axis of maximum moment of inertia by deploying masses on the tips of extendable booms in a direction perpendicular to the spin axis. A simplified model of the modified spinning Skylab is described, and analyses of the stability of motion and the rotational dynamics are presented.

MODEL DEFINITION AND EQUATIONS OF MOTION

The geometrically complex Skylab [1] (Fig. 1) is simplified to make it analytically tractable. The vehicle is modeled (Fig. 2) as a single rigid core body with principal moments of inertia I_i^* (throughout this paper, subscript i ranges from 1 through 3 and refers to the 1, 2, 3 body-fixed axes) with $I_1^* < I_3^* < I_2^*$. Attached to the core body are two flexible massless booms, each of length Γ (measured along the 2-axis in steady state) and each having a tip mass m . In the steady state, the principal moments of inertia of the entire vehicle coincide with the body-fixed axes and are designated I_i with $I_1 < I_2 < I_3$. The vehicle is assumed to have a steady-state spin velocity Ω about the 3-axis, and the angular velocity vector is written in body-fixed coordinates as $\underline{\omega} = (w_1, w_2, \Omega + w_3)$, where w_i represents small perturbations about the steady state, i.e., $|w_i| \ll 1$. Displacements u_i^k ($k = 1, 2$) of the tip masses from the spinning steady state are assumed to be small. Nonrotating boom stiffness is characterized by stiffness coefficients k_i . Structural damping is assumed proportional

SKYLAB

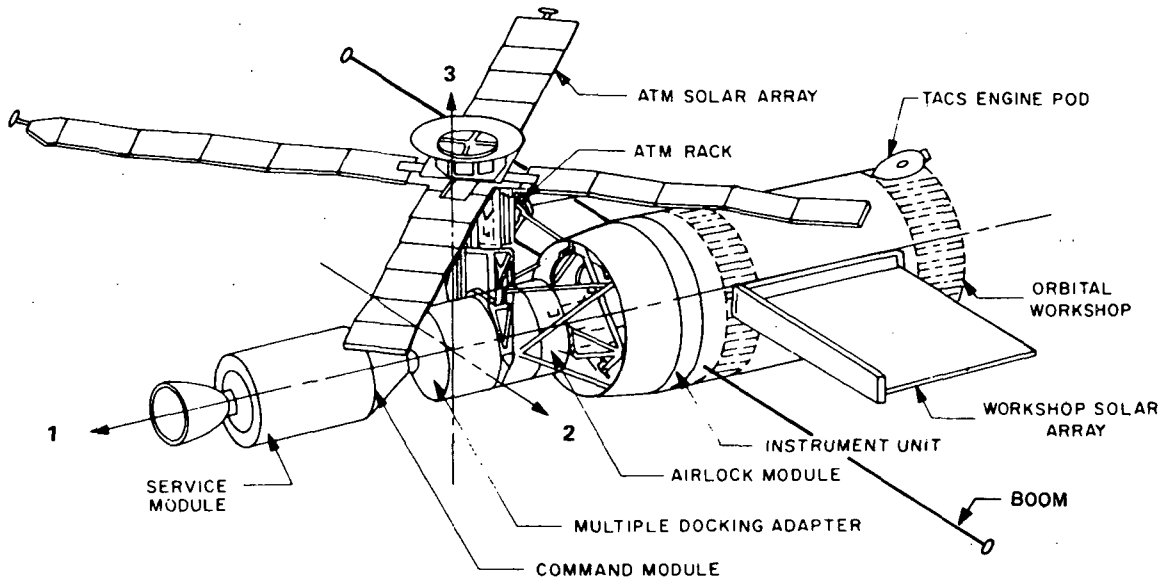


Figure 1. Skylab.

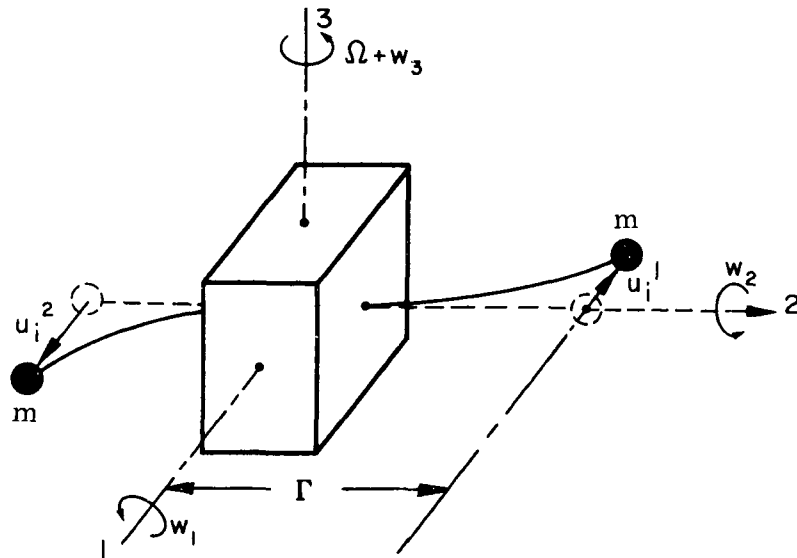


Figure 2. Simplified model.

to elastic deformation velocities and is denoted by coefficients d_i . Rotational dynamics of the vehicle may be represented by a set of nine differential equations written in variables u_i^k, w_i . The set may be reduced to six by making the substitution $u_i = u_i^1 - u_i^2$, where u_i represents the skew symmetric mode of the elastic deformations and hence causes angular motion about the vehicle's steady-state attitude. In this investigation stability of rotational motion is of interest, so only the skew symmetric mode will be considered. The corresponding linearized equations of motion are

$$\begin{aligned} w_1' - K_1 w_2 + \gamma_1 \Omega (\mu_3'' + \mu_3) &= T_1 / I_1 \Omega \\ w_2' - K_2 w_1 &= T_2 / I_2 \Omega \\ (1/\Omega) (w_1' + w_2) + \mu_3'' + \Delta_3 \mu_3 + (\sigma_3^2 + 1) \mu_3 &= 0 \end{aligned} \quad (1)$$

and

$$\begin{aligned} w_3' - \gamma_3 \Omega (\mu_1'' - 2\mu_2'') &= T_3 / I_3 \Omega \\ (-1/\Omega) w_3' + \mu_1'' + \Delta_1 \mu_1 + \sigma_1^2 \mu_1 - (1/\Gamma_2) \mu_2' &= 0 \\ (-2/\Omega) w_3 + (1/\Gamma_2) \mu_1' + \mu_2'' + \Delta_2 \mu_2 + (\sigma_2^2 - 1) \mu_2 &= 0, \end{aligned} \quad (2)$$

where

$$I_1 = I_1^* + 2m\Gamma^2$$

$$I_2 = I_2^*$$

$$I_3 = I_3^* + 2m\Gamma^2$$

$$\sigma_i^2 = k_i / m\Omega^2$$

$$\gamma_i = 2m\Gamma^2 / I_i$$

$$\Delta_i = d_i / m\Omega$$

$$K_1 = (I_2 - I_3) / I_1$$

$$K_2 = (I_3 - I_1)/I_2$$

$$\mu_i = u_i/2\Gamma$$

and T_i represents the applied torques. For physical reasons,

$$|K_k| < 1 \quad (k = 1, 2),$$

$$0 < \gamma_m < 1 \quad (m = 1, 3),$$

$$d_i > 0,$$

and

$$k_i > 0.$$

Primes represent derivatives with respect to τ , where

$$\tau = \Omega t,$$

and t denotes real time. Equations (1) describe wobble motion (resulting from angular motions about the 1- and 2-axes and linear motion in the 3-direction). Equations (2) describe in-plane motion (a combination of angular motion about the 3-axis and linear motions in the 1- and 2-directions).

STABILITY ANALYSIS

The motion of the vehicle can be described by a nutation about the axis of angular momentum which, in the absence of external torques, is inertially fixed. This motion is called passively stable if the nutation damps out and the vehicle rotates only about the axis of angular momentum (the effect of applied torques T_i is to change the attitude of this axis). The following analysis

determines under what conditions the spinning vehicle can be passively stabilized, assuming $I_1 < I_2 < I_3$.

The stability of wobble motion is investigated by obtaining the characteristic equation from equations (1):

$$(1 - \gamma_1)\lambda^4 + \Delta_3\lambda^3 - (K_1K_2 + \gamma_1K_2 + \gamma_1 - \sigma_3^2 - 1)\lambda^2 - \Delta_3K_1K_2\lambda - [(\sigma_3^2 + 1)K_1K_2 + \gamma_1K_2] = 0, \quad (3)$$

where

$$\lambda = s/\Omega = \eta + i\nu$$

and s is the Laplace operator. Regions of stability may be determined by applying the D-composition technique [2]. The stability boundary associated with the origin of the complex λ -plane is found by setting the coefficient of λ^0 equal to zero in equation (3), yielding

$$K_2 = -[(\sigma_3^2 + 1)/\gamma_1]K_1K_2. \quad (4)$$

The boundary associated with infinity on the λ -plane is found by setting the coefficient of λ^4 equal to zero:

$$\gamma_1 = 1. \quad (5)$$

The stability boundary associated with the imaginary axis of the λ -plane is found by setting λ equal to $i\nu$ in equation (3) and writing the real and imaginary parts of the result as the two equations

$$[\nu^2 - (\sigma_3^2 + 1)]K_1K_2 + \gamma_1(\nu^2 - 1)K_2 = -\nu^2[(1 - \gamma_1)\nu^2 + (\gamma_1 - \sigma_3^2 - 1)]$$

and

$$-\Delta_3\nu(K_1K_2 = -\nu^2). \quad (6)$$

Equations (6) may be solved for the relationship

$$K_2 = -K_1K_2. \quad (7)$$

Finally, a stability boundary may exist that is associated with the singular case where equations (6) are not independent; i. e., when the Jacobian J becomes identically equal to zero [2]. The Jacobian of equations (6) is

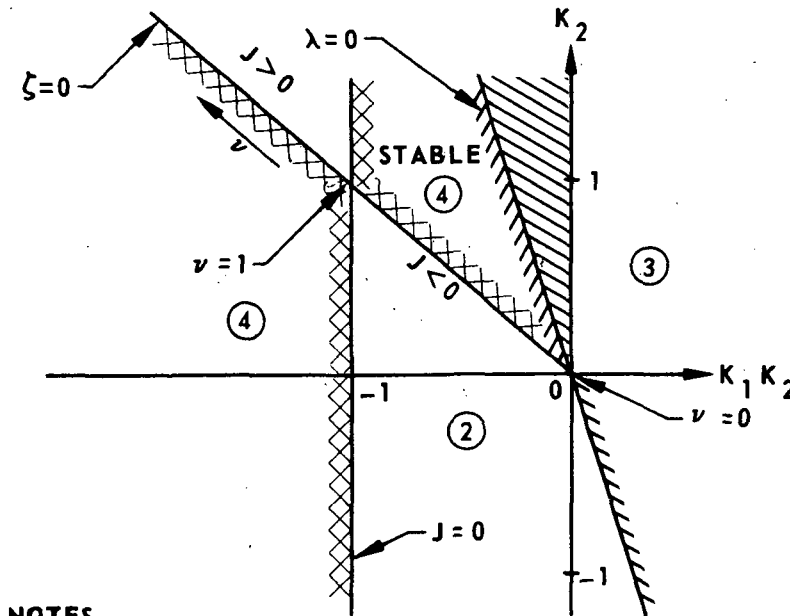
$$J = \Delta_3\gamma_1\nu(\nu^2 - 1), \quad (8)$$

which is zero when Δ_3 , γ_1 , or ν equals zero or when $\nu^2 = 1$. If $\nu^2 = 1$ is substituted into equations (6), the $J = 0$ stability boundary is found as

$$K_1 K_2 = -1. \quad (9)$$

These stability results corroborate those reported by Barbera [3].

The wobble motion stability requirements may be portrayed on a $K_1 K_2$, K_2 parameter plane (Fig. 3). The stable region may be found by considering the sign of J [2]. Double cross-hatching is used on the boundary associated with the imaginary axis (including the $J = 0$ boundary). The hatching lies on the side of the boundary that is toward the stable region; in the λ -plane, it lies on the left side of the boundary for increasing ν . If $J > 0$, the hatching in the parameter plane will also lie on the left side of the boundary as ν increases (and on the right side if $J < 0$). Single cross-hatching is used similarly on the boundary associated with the origin of the λ -plane. Continuity of cross-hatching



NOTES

1. CROSS-HATCHED REGION IS STABILITY REGION LOST BECAUSE OF FLEXIBILITY
2. ENCIRCLED NUMBERS REFER TO NUMBER OF STABLE ROOTS OF CHARACTERISTIC EQUATION
3. ADDITIONAL CONSTRAINTS: $0 < \gamma_1 < 1, \Delta_3 > 0$.

Figure 3. Stability region for wobble motion.

must exist at contour intersections in the parameter plane corresponding to the origin of the λ -plane and to other intersections where the contours have equal values of ν .

The effect of boom flexibility on stability may be assessed by considering the booms to be rigid; i. e., setting $1/\sigma_1^2$ equal to zero. The boundary of equation (4) becomes $K_1 K_2 = 0$. The stable region is thus decreased by boom flexibility, as shown by the shaded region of Figure 3. Also, the effect of boom length and tip mass may be seen by considering their effect on K_1 .

Similarly, stability of the in-plane motion may be determined by examining the characteristic equation obtained from equations (2).

$$\begin{aligned} & \lambda \{ (1 - \gamma_3) \lambda^4 + [\Delta_1 + \Delta_2 (1 - \gamma_3)] \lambda^3 \\ & + [\sigma_1^2 + \sigma_2^2 (1 - \gamma_3) + 3(1 - \gamma_3) + \Delta_1 \Delta_2] \lambda^2 \\ & + [\Delta_1 (\sigma_2^2 - 1 + 4\gamma_3) + \Delta_2 \sigma_1^2] \lambda + \sigma_1^2 (\sigma_2^2 - 1 + 4\gamma_3) \} = 0. \end{aligned} \quad (10)$$

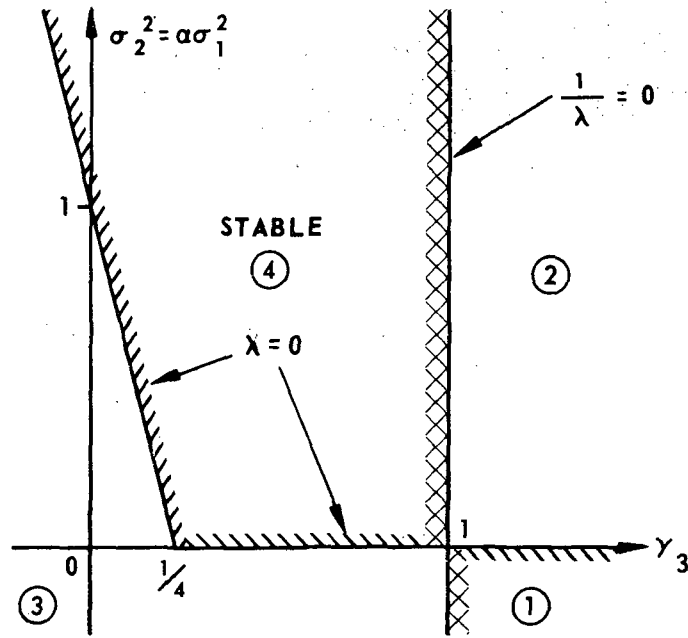
If it is assumed that the stiffness coefficient k_2 is α times as great as k_1 and k_3 , where α is a positive constant, and that $k_1 = k_3$, the application of D-decomposition to equation (10) yields the boundary associated with the origin of the λ -plane:

$$\sigma_2^2 = 0 \text{ and } \sigma_2^2 = 1 - 4\gamma_3. \quad (11)$$

The boundary associated with infinity on the λ -plane is $\gamma_3 = 1$. The boundary associated with the imaginary axis of the λ -plane yields the same two boundaries plus an additional constraint, $\Delta_1 = 0$. No additional boundaries arise from the $J = 0$ condition. The resulting region of stability is shown on a γ_3, σ_2^2 parameter plane (Fig. 4), which shows the effects of the boom characteristics on the stability of the in-plane motion.

WOBBLE MOTION DYNAMICS

Once stability has been assured, the transient dynamics of the wobble motion are of interest. The character of this motion may be investigated by using the parameter plane technique [2]. Characteristic equation (3) is used, selecting inertia ratios $K_1 K_2$ and K_2 as two adjustable parameters of interest to the designer; i. e., the effect of various values of $K_1 K_2$ and K_2 on the wobble motion dynamics will be determined. This is done by finding the relationship



NOTES:

1. SEE NOTE 2, FIG. 3
2. ADDITIONAL CONSTRAINT: $\Delta_1 > 0$

Figure 4. Stability region for in-plane motion.

between these two parameters and the roots of equation (3). The relationship may be shown by mapping a convenient contour from the λ -plane onto the $K_1 K_2$, K_2 parameter plane. The contour selected is the line

$$\lambda = -\zeta \nu_n + i \nu_n (1 - \zeta^2)^{1/2}, \quad (12)$$

where $\nu_n = \nu(1 - \zeta^2)^{-1/2}$. Any root of equation (3) lying on this contour will have a specified damping ratio ζ . This line is mapped onto the parameter plane by substituting equation (12) into equation (3), which may be written in the form

$$\sum_{p=0}^4 (a_p K_1 K_2 + b_p K_2 + c_p) \lambda^p = 0, \quad (13)$$

where values for coefficients a_p , b_p , c_p are found in Table 1.

TABLE 1. COEFFICIENTS OF WOBBLE CHARACTERISTIC EQUATION

p	a_p	b_p	c_p
0	$-(\sigma_3^2 + 1)$	$-\gamma_1$	0
1	$-\Delta_3$	0	0
2	-1	$-\gamma_1$	$1 + \sigma_3^2 - \gamma_1$
3	0	0	Δ_3
4	0	0	$1 - \gamma_1$

If λ^p is written as the sum of its real and imaginary parts,

$$\lambda^p = X_p + iY_p, \quad (14)$$

values of X_p and Y_p may be found from the recurrence formulas,

$$\begin{aligned} X_{p+1} + 2\xi\nu_n X_p + \nu_n^2 X_{p-1} &= 0, \\ Y_{p+1} + 2\xi\nu_n Y_p + \nu_n^2 Y_{p-1} &= 0, \end{aligned} \quad (15)$$

where it is seen from equations (12) and (14) that $X_0 = 1$, $Y_0 = 0$, $X_1 = -\xi\nu_n$, and $Y_1 = \nu_n(1 - \xi^2)^{1/2}$. Substituting equation (14) into equation (13) and separating the resulting real and imaginary parts, one obtains two simultaneous algebraic equations that may be solved for parameters K_1K_2 and K_2 :

$$\begin{aligned} K_1K_2 &= (B_1C_2 - B_2C_1)/J, \quad K_2 = (A_2C_1 - A_1C_2)/J, \\ J &= A_1B_2 - A_2B_1, \end{aligned} \quad (16)$$

where

$$A_1 = \sum_{p=0}^4 a_p X_p, \quad B_1 = \sum_{p=0}^4 b_p X_p, \quad C_1 = \sum_{p=0}^4 c_p X_p,$$

and

$$A_2 = \sum_{p=0}^4 a_p Y_p, \quad B_2 = \sum_{p=0}^4 b_p Y_p, \quad C_2 = \sum_{p=0}^4 c_p Y_p. \quad (17)$$

Equations (16) define the parameter plane contour corresponding to equation (12) in the λ -plane for a chosen value of ξ and coefficients a_p, b_p, c_p . Each contour is plotted as a function of the nondimensional natural frequency ν_n .

The real roots of the system may also be mapped from the λ -plane onto the parameter plane. Each selected value η of a real root is substituted for λ in characteristic equation (13). The resulting equation will define a contour on the parameter plane representing the selected location η of the real root.

The response of the system in terms of variables w_1, w_2, μ_3 may be found by casting equations (1) in the form

$$\underline{x}' = F\underline{x}, \quad (18)$$

where the vector \underline{x} is defined as

$$\underline{x} = [w_1, w_2, \mu_3, \mu_3']^T, \quad (19)$$

and the matrix F is

$$F = \frac{1}{(1 - \gamma_1)} \begin{bmatrix} 0 & (\gamma_1 + K_1) & \gamma_1 \sigma_3^2 & \gamma_1 \Delta_3 \\ K_2(1 - \gamma_1) & 0 & 0 & 0 \\ 0 & 0 & 0 & (1 - \gamma_1) \\ 0 & -(K_1 + 1) & (\gamma_1 - \sigma_3^2 - 1) & -\Delta_3 \end{bmatrix} \quad (20)$$

The response $\underline{x}(\tau)$ may then be found from

$$\underline{x}(\tau) = \phi(\tau) \underline{x}(0), \quad (21)$$

where $\underline{x}(0)$ is the initial condition vector and $\phi(\tau)$ is the state transition matrix

$$\phi(\tau) = e^{F\tau} = \mathcal{L}^{-1}\{[\lambda E - F]^{-1}\}. \quad (22)$$

Matrix E is a unit matrix of the same dimensions as the F matrix, and \mathcal{L}^{-1} represents the inverse Laplace operation. In evaluating $\phi(\tau)$, the roots of the characteristic equation (3) are the roots of the determinant $|\lambda E - F|$ and may be taken directly from the parameter plane. For example, if initial conditions exist only on w_1 and w_2 ; i. e.,

$$\underline{x}(0) = (x_{10}, x_{20}, 0, 0)^T, \quad (23)$$

the $w_1(\tau)$ response is found from

$$w_1(\tau) = \mathcal{L}^{-1}[\Phi_{11}(\lambda)x_{10} + \Phi_{21}(\lambda)x_{20}], \quad (24)$$

where

$$\begin{aligned} \Phi_{11}(\lambda) &= \lambda[\lambda^2 + \Delta_3\lambda/(1 - \gamma_1) + (1 + \sigma_3^2 - \gamma_1)/(1 - \gamma_1)]/|\lambda E - F|, \\ \Phi_{21}(\lambda) &= K_2\Phi_{11}(\lambda)/\lambda. \end{aligned} \quad (25)$$

Example

The model described by equations (1) and (2) may be used to crudely represent a spinning Skylab. Representative values for the coefficients in equation (3) are given in Table 2.

TABLE 2. PHYSICAL CHARACTERISTICS OF SKYLAB

$I_1^* = 1.01 \times 10^6 \text{ kg m}^2$	$\Gamma = 23.3 \text{ m}$	$k_2 = 7.4 \times 10^4 \text{ N/m}$
$I_2^* = 6.90 \times 10^6 \text{ kg m}^2$	$m = 227 \text{ kg}$	$d_i = 0.04 (k_i m)^{1/2}$
$I_3^* = 6.85 \times 10^6 \text{ kg m}^2$	$k_1 = k_3 = 146 \text{ N/m}$	$\Omega = 0.6 \text{ s}^{-1}$

If the values are substituted into equations (16), ξ -contours may be plotted on the K_1K_2 , K_2 parameter plane as functions of ν_n (Fig. 5). Stability boundaries defined by equations (4), (7), and (9) are also plotted in Figure 5. Real root boundaries are found to be outside the stable region and hence are of no interest in the Skylab problem.

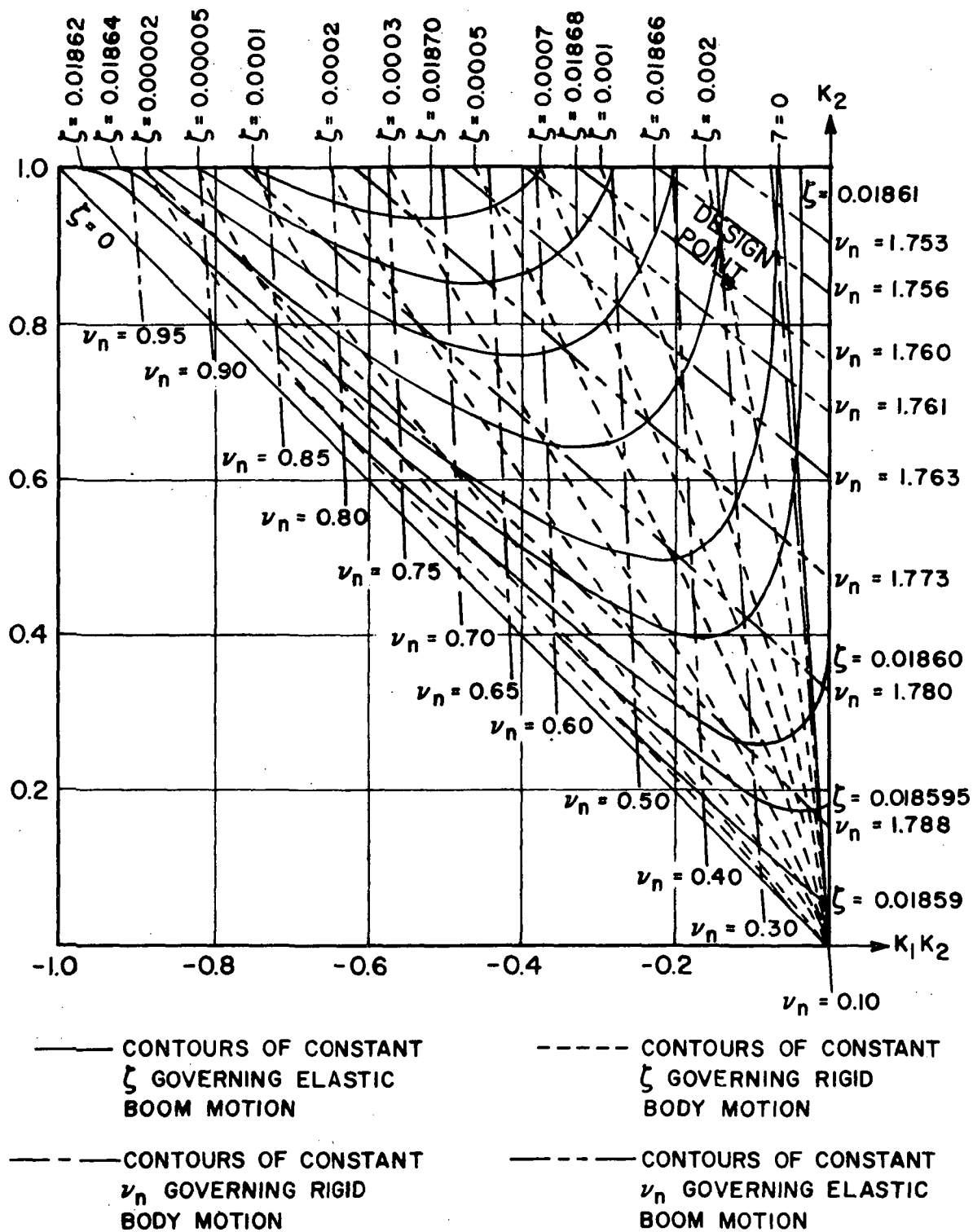


Figure 5. K_2 versus K_1K_2 parameter plane plot.

A typical design point for Skylab is shown on the parameter plane. It corresponds to the physical characteristics shown in Table 2. The corresponding roots of the characteristic equation are seen to have damping ratios (ζ) and nondimensional natural frequencies ν_n of

$$\zeta = 0.002, \quad \nu_n = 0.2854$$

and

$$\zeta = 0.01863, \quad \nu_n = 1.7612. \quad (26)$$

If the values of Table 2 and equations (26) are substituted into equation (21), the response for the Skylab model is found. For example, from equation (24),

$$\begin{aligned} w_1(\tau) = & 1.0978 e^{-0.0005672\tau} \cos(0.2854\tau + 0.3274)w_1(0) \\ & + 0.09359 e^{-0.03281\tau} \cos(1.761\tau + 4.1270)w_2(0), \end{aligned} \quad (27)$$

where $\underline{x}(0)$ is defined by equation (23). For $w_1(0) = w_2(0) = 0.001$, the response $w_1(\tau)$ is plotted in Figure 6. Similarly $w_2(\tau)$ and $\mu_3(\tau)$ are also determined and shown in Figures 7 and 8.

CONCLUSION

It has been shown that it is possible to passively stabilize the motion of a simplified model of a spinning Skylab by deploying flexible booms, thus altering the moments of inertia. Analytical results indicate the required boom stiffness properties for given vehicle mass properties and spin rates to achieve passive stability. Further, the use of the simplified model leads to results amenable to physical interpretation.

To gain confidence that these results will apply to the actual Skylab, an additional step is being implemented. A detailed digital simulation model of the spinning Skylab vehicle has been developed at the Marshall Space Flight Center, and results compare favorably with those of the simplified model.

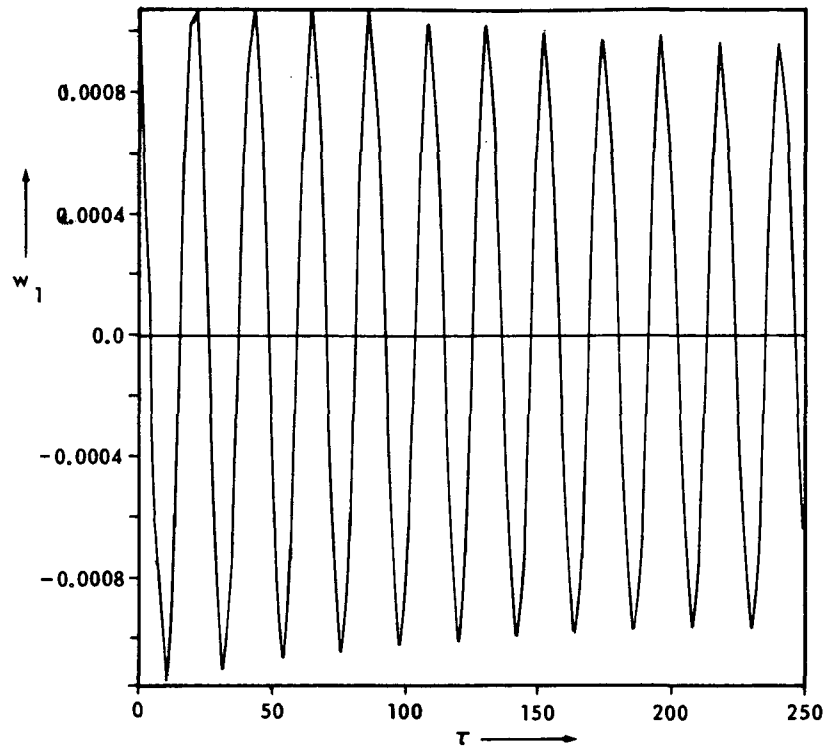


Figure 6. w_1 versus τ .

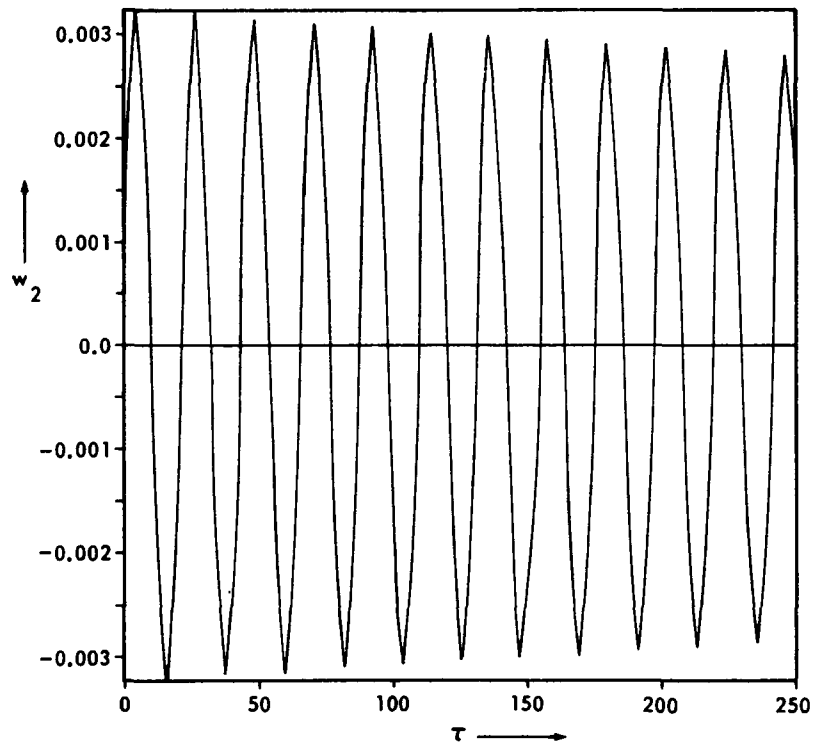


Figure 7. w_2 versus τ .

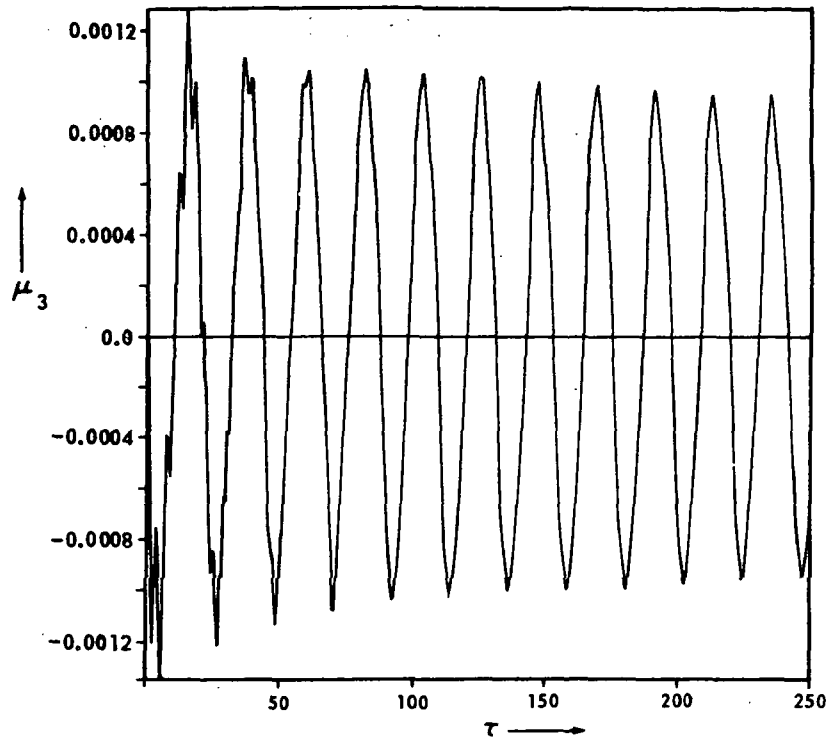


Figure 8. μ_3 versus τ .

REFERENCES

1. Chubb, W. B.; and Seltzer, S. M.: *Skylab Attitude and Pointing Control System*. NASA TN D-6068, 1971.
2. Siljak, D. D.: *Nonlinear Systems*. John Wiley & Sons, Inc., New York, 1969, pp. 455-457, 404-406, 33-37, 4-51.
3. Barbera, F. J.: *Attitude Stability of Spinning Flexible Spacecraft*, Ph.D. Dissertation, University of California, Los Angeles, Dec. 1971.

APPROVAL

PASSIVE STABILITY OF A SPINNING SKYLAB

By S. M. Seltzer

The information in this report has been reviewed for security classification. Review of any information concerning Department of Defense or Atomic Energy Commission programs has been made by the MSFC Security Classification Officer. This report, in its entirety, has been determined to be unclassified.

This document has also been reviewed and approved for technical accuracy.

Hans H. Hoesenthién

HANS H. HOSENTHIEN
Chief, R&D Analysis Office

F. B. Moore

F. B. MOORE
Director, Astrionics Laboratory

DISTRIBUTION

INTERNAL

DIR	S&E-P-DIR	
	Mr. Kroeger	S&E-ASTR-M
DEP-T		Mr. Boehm
	S&E-ASTN-AD	
PD-DIR	Mr. Farrow	S&E-ASTR-S
Dr. Murphy	Mr. Bullock	Mr. Wojtalik
	Mr. Holland	Mr. Brooks
PD-DO-DIR		Mr. Scofield
Dr. Thomason	S&E-ASTR-DIR	Mr. Chubb
	Mr. Moore	Mr. Justice
PD-DO-E	Mr. Powell	Mr. Valley
Mr. Schultz		Mr. Tanner
	S&E-ASTR-A	
PM-HE-MGR	Mr. Hcsenthien	S&E-CSE-DIR
Dr. Speer	Dr. Borelli	Dr. Haeussermann
	Dr. Nurre	
S&E-DIR	Dr. Clarke	S&E-CSE-I
Mr. Weidner	Mr. Kennel	Mr. Hammer
Mr. Richard	Mr. Jones	
	Mr. von Pragenau	AD-S
S&E-AERO-DIR	Mr. Carroll	Dr. Stuhlinger
Dr. Geissler	Miss Flowers	
Mr. Horn	Dr. Seltzer (20)	A&TS-MS-H
		A&TS-MS-IL (8)
S&E-AERO-D	PM-SI-MGR	A&TS-MS-IP (2)
Dr. Lovingood	Mr. Hardy (2)	
Dr. Worley		A&TS-PAT
Dr. Glaese	S&E-ASTR-G	Mr. L. D. Wofford, Jr.
	Mr. Mandel	
S&E-AERO-G	Dr. Doane	A&TS-TU
Mr. Baker	Dr. Campbell	Mr. Winslow (15)
	PD-DO-E	
PM-PR-M	Mr. Digesu	

EXTERNAL

University of Santa Clara	University of California, San Diego
Electrical Engineering Department	P.O. Box 109
Santa Clara, California 95053	La Jolla, California 92037
Attn: Prof. Dragoslav Siljak	Attn: Prof. Robert Roberson
Scientific and Technical Information Facility (5)	Auburn University
P. O. Box 33	Electrical Engineering Department
College Park, Maryland 20740	Auburn, Alabama 36830
Attn: NASA Representative (S-AK/RKT)	Attn: Prof. C. L. Phillips
U.S. Army Missile Command	U.S. Naval Postgraduate School
Redstone Arsenal, Alabama 35809	Monterey, California 93940
Attn: Mr. Jess Huff, RG	Attn: Prof. Sydney Parker
Mr. James McLean, RGN	Prof. George Thaler
NASA	Dr. Gerhard Schweitzer
Washington, D.C. 20546	Akadem. Oberrat, Institut B fuer
Attn: Mr. Melvin F. Markey, MTG	Mechanik, Technische Universitaet
Mr. Jerome Malament, MTG	Muenchen, Germany
Dr. Peter Kurzhals, REG	
Mr. Robert Lovelett, MF	Professor Bernard Asner, Jr.
	Mathematics Department
University of California, Los Angeles	Bogazici Universitesi
4731-D Boelter Hall	Istanbul, Turkey
Los Angeles, California 90024	
Attn: Prof. Peter Likins	
Mr. Frank J. Barbera	